Development 138, 3307-3317 (2011) doi:10.1242/dev.066241

Barx2 and Fgf10 regulate ocular glands branching morphogenesis by controlling extracellular matrix remodeling

Cindy Tsau[1], Masataka Ito[2], Anastasia Gromova[1,3], Matthew P. Hoffman[4], Robyn Meech[5,*] and Helen P. Makarenkova[1,3,*,†]

SUMMARY

The lacrimal gland (LG) develops through branching morphogenesis and produces secretions, including tears, that lubricate and protect the ocular surface. Despite the prevalence of LG disorders such as dry eye, relatively little is known about the regulation of LG development. In this study, we show that the homeobox transcription factor Barx2 is highly expressed in conjunctival epithelium, eyelids and ocular [lacrimal, harderian (HG), and meibomian (MG)] glands and is necessary for normal ocular gland and eyelid development. Barx2$^{-/-}$ mice show defective LG morphogenesis, absence of the HG, and defects in MG and eyelid fusion. Ex vivo antisense assays confirm the requirement for Barx2 in LG bud elongation and branching. Gene expression profiles reveal decreased expression of several adhesion and matrix remodeling molecules in Barx2$^{-/-}$ LGs. In culture, Barx2 regulates expression of matrix metalloproteinases (MMPs) and epithelial cell migration through the extracellular matrix. Fibroblast growth factors are crucial regulators of LG development and we show that Barx2 is required for Fgf10-induced LG bud elongation and that both Barx2 and Fgf10 cooperate in the regulation of MMPs. Together, these data suggest a mechanism for the effects of loss of Barx2 on ocular gland development. Intriguingly, salivary glands that also express a high level of Barx2 develop normally in Barx2$^{-/-}$ mice and do not show altered levels of MMPs. Thus, the function of Barx2 is specific to ocular gland development. Based on our data, we propose a functional network involving Barx2, Fgf10 and MMPs that plays an essential role in regulating branching morphogenesis of the ocular glands.

KEY WORDS: Barx2, Fgf10, Harderian gland, Lacrimal gland, Meibomian glands, Submandibular gland, Mouse

INTRODUCTION

Branching morphogenesis is a fundamental process involved in the development of a number of vertebrate and invertebrate organs, such as the *Drosophila* tracheal system, kidney, lung, mammary glands, salivary glands and the major ocular glands: lacrimal (LG), meibomian (MG) and harderian (HG) glands (Dudley et al., 1999; Hogan et al., 1997; Knop et al., 2011; Lu et al., 2006; Metzger and Krasnow, 1999; Monte et al., 2007; Patel et al., 2006). Branching morphogenesis involves specification of the epithelium and induction and elongation of a primary bud, followed by development of the mature organ through repetitive bud elongation and cleft formation (Sakai, 2009). Many of the key mechanisms that underlie these processes appear to be conserved among all branched organs; however, structural and functional differences between organs also suggests the existence of organ-specific regulatory mechanisms.

We and others have shown that the homeodomain transcription factor Barx2, which is related to the *Drosophila* Bar family genes, is expressed in several epithelial tissues that develop through branching morphogenesis such as lung, kidney, mammary gland, and lacrimal and salivary gland primordia (Herring et al., 2001; Jones et al., 1997; Olson et al., 2005; Sander et al., 2000; Sellar et al., 2001; Sellar et al., 2002; Stevens and Meech, 2006). However, the role of Barx2 during branching morphogenesis has not been determined.

Murine LG development begins on embryonic day (E) 13.5 as a tubular invagination of the conjunctival epithelium at the temporal extremity of the eye (Makarenkova et al., 2000). After a period of elongation, the LG bud invades the mesenchymal sac at E16.5 and begins a period of rapid growth and branching to form prospective lobular structures: the intra- and ex-orbital lobes. During the postnatal period, LGs continue to branch and differentiate and by the time of eye re-opening 7 days after birth (P7) they have begun to produce a secretion containing mucins, lipids, lysozyme and immunoglobulins (Franklin, 1989), which lubricates and protects ocular surfaces (Wang et al., 1995). In humans, the LG consists of an orbital (or superior) portion and a small palpebral (or inferior) portion of acinar morphology. MGs are located in the eyelid in both humans and rodents. In mice, these modified sebaceous glands originate from the eyelid margin at E18.5 and produce oil (meibum) that helps to prevent tear film from evaporating (Nien et al., 2010). The protection of ocular surfaces in rodents is also mediated by the HG, which is located within the orbit. The HG originates from the nasal part of the conjunctival epithelium at E16 and forms a branched structure behind the eyeball. In contrast to the acinar morphology of the LG, the HG has a tubulo-alveolar organization and is composed exclusively of one type of secretory cell (Payne, 1994). The mature HG is the largest ocular gland in rodents (Payne, 1994) and it secretes lipids, melatonin and porphyrins, the role of which in protection of ocular surface is not completely clear (Satoh et al., 1996; Villapando et al., 2005). In primates, the HG is either absent or vestigial.

[1]The Neurosciences Institute, San Diego, CA 92121, USA. [2]Department of Developmental Anatomy and Regenerative Biology, National Defense Medical College, 3-2 Namiki, Saitama, Japan 359-8513. [3]The Scripps Research Institute, La Jolla, CA 92037, USA. [4]Laboratory of Cell and Developmental Biology, National Institute of Dental and Craniofacial Research, National Institutes of Health, Bethesda, MD 20892, USA. [5]Department of Clinical Pharmacology, Flinders University, Bedford Park, South Australia 5042, Australia.

*These authors contributed equally to this work
[†]Author for correspondence (hmakarenk@scripps.edu)

Accepted 24 May 2011

The structure of ocular glands has been studied extensively; however, the regulation of their development and differentiation is still not well understood. Fibroblast growth factor 10 (Fgf10) is involved in induction of both LGs and HGs (Govindarajan et al., 2000; Makarenkova et al., 2000). The induction and outgrowth of the LG bud involves the localized activation of a signaling cascade involving N-deacetylase/N-sulfotransferase (heparan glucosaminyl) that modifies heparan sulfate (HS), FGF receptors and Src homology 2-containing tyrosine phosphatase 2 (Pan et al., 2008). Recently, we showed that the pattern of branching is controlled by changes in the FGF gradient, and that interactions between growth factors and HS regulate both the shape of the morphogenetic gradient and downstream cellular responses. This suggested distinct roles for FGF gradient formation and receptor affinity in regulating branching morphogenesis (Makarenkova et al., 2009).

Fgf10 also cooperates with the homeobox transcription factor Pax6, which is expressed in LG epithelium (Makarenkova et al., 2000). Pax6 is one of the earliest factors required for LG development, as shown by the defects in LG structure observed even in heterozygous small eye (*Sey*) mice that carry a *Pax6* mutation (Makarenkova et al., 2000). FGFs regulate the expression of another homeodomain protein, *Six1*, which is necessary for ocular placode induction and is important for normal LG development (Ahrens and Schlosser, 2005; Chen et al., 2009; Laclef et al., 2003). These studies suggest that primary bud induction and branching morphogenesis of ocular glands occurs through functional interaction of FGFs with transcription factors that are expressed in spatially restricted patterns during development. Defining these interactions is essential to understanding the mechanisms that regulate ocular gland development.

In the present study, we show that the Barx2 homeobox protein is necessary for normal LG and HG development and that it is also involved in eyelid fusion and MG patterning. HGs were absent and LGs were significantly reduced or malformed in *Barx2* null mice. Barx2 is required for FGF-mediated LG bud elongation, and Barx2 and Fgf10 regulate the expression of matrix metalloproteinases (MMPs) that are required for epithelial bud outgrowth, providing a mechanism for the effects of loss of Barx2 on ocular gland development. Salivary glands also express a high level of Barx2 during development; however, *Barx2* null salivary glands develop normally, suggesting that Barx2 has a specific role in ocular gland development. We propose that a functional network involving Barx2, Fgf10 and MMPs plays an essential role in regulating branching morphogenesis of the ocular glands.

MATERIALS AND METHODS

Mice

Barx2-null mice were obtained from Dr Geoff Rosenfeld (University of California, San Diego, CA, USA). The sequences encoding the homeodomain and C-terminal region of *Barx2* were deleted and the 134 amino acid N-terminal Barx2 region was fused in frame to β-galactosidase (Olson et al., 2005). Mice were genotyped by genomic PCR (Olson et al., 2005). *lacZ* expression in $Barx2^{-/-}$- and $Barx2^{+/-}$-*lacZ* knock-in mice and *Pax6-lacZ* transgenic mice (Makarenkova et al., 2000) was assessed by β-galactosidase histochemistry using established protocols (Dean et al., 2004; Faber et al., 2002; Song et al., 1996). In addition, CD1 mice (Jackson Laboratories) were used for preparation of LG explant cultures.

Histology, LG immunostaining and microscopy

Paraffin sections were prepared and stained with Hematoxylin and Eosin using conventional methods. Whole-mount immunostaining used rabbit polyclonal antibodies to Barx2 (M-186, Santa Cruz Biotechnologies), Mmp2 and Mmp9 (RP3-MMP-2 and RP3-MMP-9, Triple Point Biologics). Images of whole glands were taken under a Leica MZ-FLII microscope. Confocal images were acquired using a Bio-Rad (Zeiss) Radiance 2100 Rainbow laser scanning confocal microscope. Images were analyzed using Imaris software (Bitplane Scientific Software).

LG epithelial explant culture: FGF-treatment and antisense treatment

LGs were dissected from E15.5 and E16.5 embryos and grown as described previously (Makarenkova et al., 2000). To study epithelial responses to Fgf10, an Fgf10 loaded bead was placed near the explant (Makarenkova et al., 2009) and bud growth was monitored for 24-72 hours. For *Barx2* knockdown, *Barx2* antisense and control morpholino oligodeoxynucleotides (ODNs) (Gene Tools, Corvalis, OR, USA) (Meech et al., 2005) were complexed with Lipofectamine 2000 (Invitrogen), diluted with 25% Pluronic gel to 5 μM, vortexed and kept on ice (Becker et al., 1999; Makarenkova and Patel, 1999; Makarenkova et al., 2000). A 10 μl drop of ODNs was placed on each LG explant (Makarenkova et al., 2000). Cultures were maintained for 48-72 hours and ODNs replaced every 8-10 hours to increase transfection efficiency. Differences in the number of branches in control and antisense-treated explants were assessed using the nonparametric Wilcoxon signed rank test (Ostle, 1975). $P<0.01$ was considered to reflect a statistically significant difference.

Gelatin zymography and migration assays

Zymography was performed using both LG buds (E15.5) and A253 epithelial cells (ATCC). Equal numbers of $Barx2^{-/-}$ and $Barx2^{+/+}$ LG buds were grown in growth factor-reduced Matrigel (BD Biosciences) in four-well dishes, covered with 100 ml of serum-free media. After 24 hours at 37°C, the conditioned media was subjected to zymography using 10% gels containing 0.1% gelatin according to the manufacturer's protocol (Invitrogen). A253 cells were maintained in DMEM with 10% FBS and glutamine and transfected with pcDNA3 or pcBarx2 expression plasmids using the Amaxa Nucleofector System (Lonza). Cells (4×10^5) were mixed with 3 mg/ml Matrigel, overlaid with serum-free media and incubated for 48 hours at 37°C. The conditioned media was subjected to gelatin zymography.

For migration assays, A253 cells were transfected with pcDNA3 or pcBarx2 expression plasmids using Lipofectamine and grown for 24 hours. Polycarbonate filter Transwells (8 μm pore size; Corning-Costar) were filled with 3 mg/ml Matrigel and overlaid with 1×10^4 cells in CMRL-defined media. Fibronectin (20 mg/ml) was added to the media below the inserts as an attractant. After 24 hours at 37°C, cells were stained with 0.2% Cresyl Violet and cells that had migrated to the under surface of the filter were counted.

MMP inhibitors

The broad MMP inhibitor 3-(N-hydroxycarbamoyl)-(2R)-isobutylpropionyl-L-tryptophanmethylamide (GM6001) was dissolved at 100 mM in dimethylsulfoxide (DMSO) and added to explanted E15.5 LGs at a final concentration of 10 μM (Gijbels et al., 1994; Grobelny et al., 1992). GM6001 has an affinity (K_I) of 27 nM against Str1, 0.4 nM against skin fibroblast collagenase, 0.5 nM against gelatinase A, 0.2 nM against gelatinase B and 0.1 nM against neutrophil collagenase (Galardy et al., 1994a; Galardy et al., 1994b).

Chromatin immunoprecipitation (ChIP)

ChIP was performed as described previously (Stevens et al., 2004). Briefly, E17.5-18.0 LGs were fixed with paraformaldehyde, minced with equivalent amounts of pre-cleared cross-linked chromatin and precipitated with 5 μg of polyclonal rabbit Barx2 antibody (M-186; Santa Cruz Biotechnology) or preimmune rabbit serum and captured with Protein A beads. Enrichment of genomic DNA corresponding to the Mmp2 promoter region was determined by PCR using Mmp2 promoter-specific primers (forward, 5′-CAACTCTGTTCAGGCAGGTGA-3′; reverse, 5′-GGAAA-TGTGTGTTCTGCTCCCA-3′) and quantified by gel densitometry.

RT PCR

LGs and submandibular glands (SMG) were dissected as described (Makarenkova et al., 2000; Patel et al., 2008; Steinberg et al., 2005) and RNA prepared using Trizol reagent (Invitrogen), treated with DNase using the DNA-free kit (Ambion) and reverse transcribed using random primers

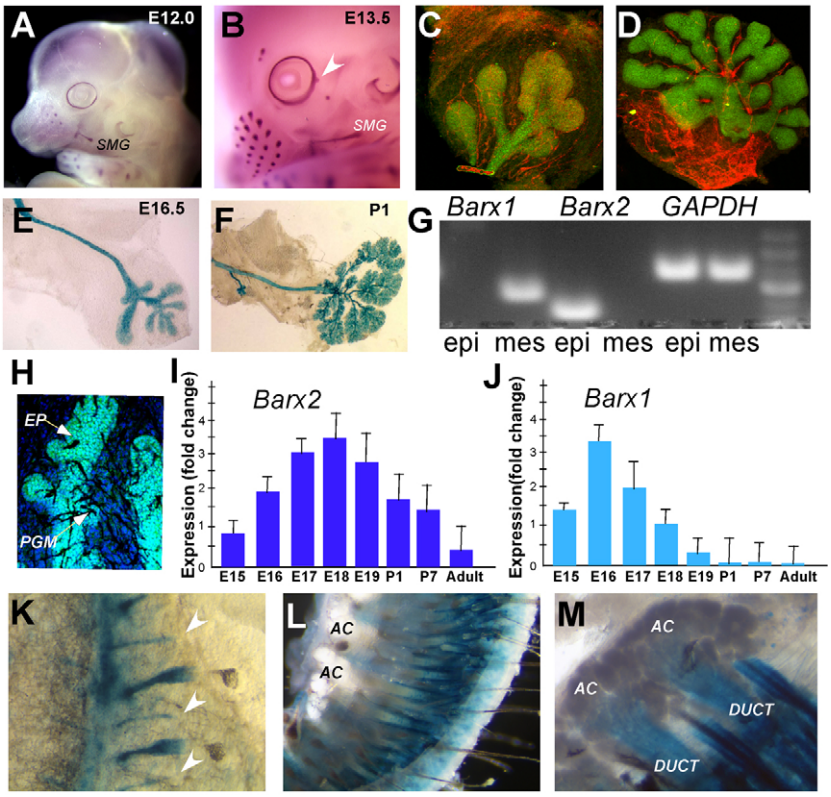

Fig. 1. Barx2 expression in the mouse embryo and ocular glands. (**A**,**B**) In situ hybridization showing Barx2 expression in the mouse embryo at E12.0 (A) and at E13.5 (B) in the conjunctival epithelium, in the primary lacrimal bud (white arrowhead), and submandibular gland primordium (SMG). (**C**,**D**). Barx2 (green) and CD31 (red) immunostaining of an E16.5 lacrimal gland (LG; C). The LG was isolated at E16.0 and cultured for an additional 30 hours (D). Barx2 is in the epithelial component of the gland and CD31 in blood vessels. (**E**,**F**). *Barx2-lacZ*-driven β-galactosidase expression in the epithelial component of E16.5 (E) and P1 (F) *Barx2*$^{+/-}$ LGs. (**G**) RT-PCR analysis of isolated epithelial and mesenchymal components of the LG. *Barx1* is expressed only in mesenchyme (mes) and *Barx2* is expressed only in epithelium (epi). (**H**) Barx2 protein expression (green) in the HG at P2. Nuclei were stained with DAPI (blue). EP, epithelium; PGM, pigment cells. (**I**,**J**) Quantitative RT-PCR analysis of *Barx2* (I) and *Barx1* (J) expression relative to the E15.5 stage and normalized to 18S ribosomal RNA. LGs throughout embryonic and postnatal development and in the adult mouse. Error bars represent s.d. (**K-M**) *Barx2-lacZ*-driven β-galactosidase expression in meibomian glands (MGs). At P3.5 (K), MGs are visible as the tubular invaginations of epidermis (arrowheads). In P30 eyelids (L,M), Barx2 is expressed only in ductal (DUCT) but not acinar (AC) components of the gland. M is higher magnification.

and MMluV reverse transcriptase (New England Biolabs). Semi-quantitative RT-PCR reactions were performed using HotMasterTaq (Eppendorf), resolved on agarose gels and band intensity was measured using AlphaEase software. Quantitative RT-PCR was performed using the Applied Biosystems 7300 (ABI 7300) Real-Time PCR System.

Primer sequences were as follows: *Gapdh*: forward 5′-TGTCTTCACCACCATGGAGAAGGC-3′, reverse 5′-TGGCAGTGATGGCATGGAACTGTGG-3′; *Barx2*: forward 5′-TTTGTCTACCCCAGACAGGTTG-3′, reverse 5′-TCAATCTCCTCTGATGTGGGAAT-3′; *Mmp2*: forward 5′-AGACAGGTGACCTTGACCAGAAC-3′, reverse 5′-ATACTTTTAAGGCCCGAGCAAAA-3′; *Mmp3*: forward 5′-CCCACCAAGTCTAACTCTCTGGA-3′, reverse 5′-ATCCATGTTGGATGGAAGAGATG-3′; *Mmp9*: forward 5′-AAGACCTGAAAACCTCCAACCTC-3′, reverse 5′-GTGTTCGAATGGCCTTTAGTGTC-3′; *Timp2*: forward 5′-AAGGACCTGACAAAGACATCGAG-3′, reverse 5′-GCTCTTCTTCTGGGTGATGCTAA-3′; *Timp3*: forward 5′-CCTTTGGCACTCTGGTCTACACT-3′,reverse, 5′-ACCTCTCCACAAAGTTGCACAGT-3′; m*Timp4*: forward 5′-TGGTGTGAAGCTAGAAACCAACA-3′, reverse 5′-AGATGGTACATGGCACTGCATAG-3′.

For RT-PCR array analysis, cDNA was prepared using the RT² First Strand Kit according to the manufacturer's protocol (SABiosciences) and applied to the Mouse Extracellular Matrix and Adhesion Molecules RT²Profile PCR Array (SABiosciences). Amplification used the RT2 SYBR Green/ROX qPCR Master Mix and the 7300 Real-Time PCR System. Relative gene expression was determined using ΔΔCt method and PCR array data analysis software.

RESULTS

Barx2 is expressed in the epithelial component of the developing LG and HG

Both LGs and HGs originate from the conjunctival epithelium (Govindarajan et al., 2000; Makarenkova et al., 2000); we previously showed that conjunctival epithelium and LG primordium express Barx2 (Meech et al., 2005), suggesting that developing LGs and HGs might also express Barx2.

The pattern of Barx2 expression was determined using in situ hybridization, Barx2-β-galactosidase histochemistry and immunostaining. At E12.0, Barx2 mRNA was expressed in the conjunctival epithelium and later (at E13.5) in the primary lacrimal bud (Fig. 1A,B). Barx2 was also expressed in hair follicles and SMG primordium (Fig. 1A,B). At E16-16.5, Barx2 protein was detected in LGs by immunostaining (Fig. 1C,D) and by β-galactosidase histochemistry in heterozygous *Barx2-lacZ* knock-in mouse embryos (Olson et al., 2005) (Fig. 1E). Barx2 remained highly expressed in the elaborated LG of P1 pups (Fig. 1F). Barx2 was also found in the epithelial part of the HG (Fig. 1H).

At all stages and using all detection methods, Barx2 appeared only in the epithelial component of the LG. To confirm this restricted pattern, Barx2 was measured by RT-PCR in enzymatically separated E16.5 LG epithelial and mesenchymal components. Barx2 expression was detected only in the epithelial component of the gland (Fig. 1G). By contrast, Barx1 expression was detected only in the mesenchyme (Fig. 1G). Thus, Barx1 and Barx2 have a reciprocal pattern of expression during LG development. Spatiotemporal expression of Barx2 and Barx1 in whole LGs was studied from E15.5 until P7 and in adult using real-time RT-PCR. Barx2 was expressed throughout LG development with the highest level of expression at E17-19, which would be consistent with a role for Barx2 in LG branching and maturation (Fig. 1I). Barx2 expression decreased in the LG during postnatal development. By contrast, the highest level of Barx1 mRNA was detected earlier in development (~E16-17), a stage likely to be associated with extensive remodeling of mesenchyme (Fig. 1J), and its expression had decreased substantially by E18-19.

Barx2 is expressed in MGs

MGs are located at the rim of the eyelids; their development starts at E18.5 and by P3 they appear as a cord of epithelium between the eyelash follicles (Nien et al., 2010). Barx2 was expressed in these

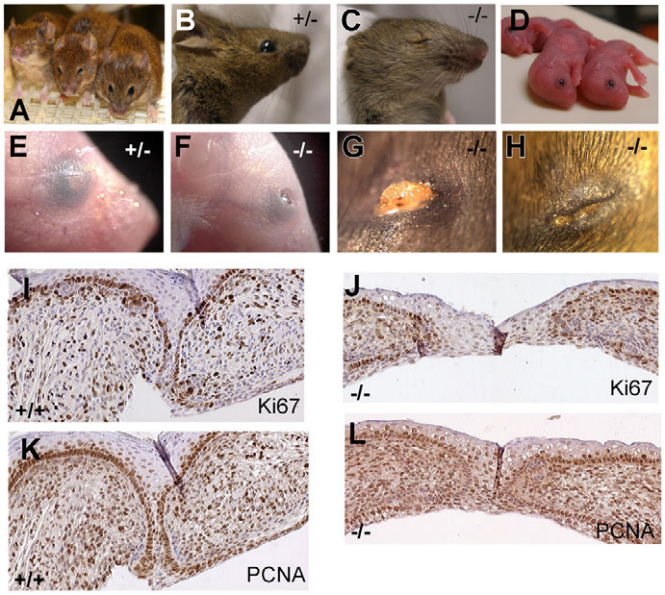

Fig. 2. The *Barx2* null mouse has defects in eyelid development. (**A**) Variation in eye size in *Barx2*$^{-/-}$ mice. From left to right: *Barx2*$^{-/-}$ mouse with no external eyes, small eyes, and almost normal eye size. (**B**) Adult (12 weeks of age) *Barx2*$^{+/-}$ mouse with normal eyes. (**C**) Adult (12 weeks of age) *Barx2*$^{-/-}$ mouse with fused eyelids. (**D**) Newborn *Barx2*$^{-/-}$ mice with the 'open-eye' defect. (**E**) *Barx2*$^{+/-}$ P4 mouse with a normally fused eyelid. (**F**) *Barx2*$^{-/-}$ P4 littermate with a partially open eyelid. (**G**) Cyst-like corneal growth on the eye of a P14 *Barx2*$^{-/-}$ mouse. (**H**) P14 Barx2$^{-/-}$ mouse with irregular fused eyelid. (**I-L**) Histological analysis of wild-type eyelids at E16.5 (I,K) shows extensive overlap of the extending lids and the beginning of lid fusion. *Barx2*$^{-/-}$ eyelids (J,L) show delayed extension, little overlap and no fusion. Immunostaining with Ki67 (I,J) or PCNA (K,L) antibody (brown nuclei) shows little difference in cell proliferation between wild-type and *Barx2*$^{-/-}$ eyelids.

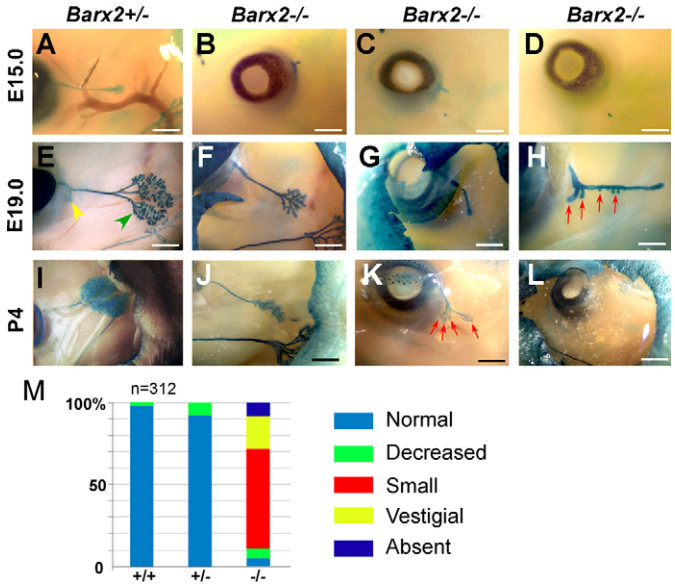

Fig. 3. The *Barx2* null mouse has striking defects in lacrimal gland (LG) development. (**A-D**) The primary lacrimal bud of an E15.0 *Barx2*$^{+/-}$ embryo shows normal extension (A). By contrast, lacrimal buds of *Barx2*$^{-/-}$ embryos show little extension (B,C) and are sometimes absent (D). (**E**) The LG of an E19.0 *Barx2*$^{+/-}$ embryo is well branched and is represented by both exorbital (green arrowhead) and intraorbital (yellow arrowhead) lobes. (**F-H**) By contrast, LGs of E19.0 *Barx2*$^{-/-}$ littermates have not formed the intraorbital lobe and are poorly branched (F) or unbranched (G) and, in some cases, ectopic buds (red arrows in H) appear from the proximal part of the duct. (**I-L**) The LG of a P4 *Barx2*$^{+/-}$ mouse is well branched, whereas LGs of *Barx2*$^{-/-}$ mice are poorly branched (J), vestigial (K, red arrows) or missing (L). (**M**) Analysis of LG phenotypes in *Barx2*$^{+/+}$, *Barx2*$^{+/-}$ and *Barx2*$^{-/-}$ E19.0 embryos (*n*=312 LGs).

epithelial cords as well as in eyelash follicles (Fig. 1K). In adult (P30) MGs, Barx2 expression was found only in the main ductal and not the acinar region (Fig. 1L,M).

Barx2$^{-/-}$ mice show eyelid fusion defects

Barx2$^{-/-}$ mice (Olson et al., 2005) showed multiple defects of ocular gland and eyelid development (Figs 2, 3). The development of mouse eyelids starts at E13.0-13.5, and complete eyelid closure is accomplished by E16.0-16.5. Eyelid folds extend from each edge of the eye over the cornea towards the center of the eye where they fuse. Eyelids form a protective barrier that is crucial for normal eye development especially during the first postnatal week when the ocular glands are still not functionally differentiated. Approximately 80% of E17.0 *Barx2*$^{-/-}$ embryos (11 litters examined; $P<0.01$) showed eyelid fusion defects (Fig. 2F), whereas *Barx2*$^{+/-}$ and *Barx2*$^{+/+}$ embryos had normally fused eyelids by E16.0 (Fig. 2E). Similar to a previous report (Olson et al., 2005), ~50% of *Barx2*$^{-/-}$ mice were born with open or partially open eyes (12 litters examined; $P<0.01$) (Fig. 2D). The eyelid fusion delay also seemed to be associated with a delay in eye re-opening in older pups. Eyelid closure and re-opening defects appeared to be associated with abnormal eye phenotypes in adult *Barx2*$^{-/-}$ mice, such as a 'smaller eye' or a slit eye phenotype (Fig. 2A-C). Ocular surface phenotypes observed in a subset of mice included inflammation (blepharitis and conjunctivitis), abnormal eyelid and corneal keratinization, and corneal epithelial defects (Fig. 2G,H). In general, mice with inflammation were more likely to have small, vestigial or absent LGs than mice without inflammation, suggesting that ocular surface damage might also be related to impaired lubrication due to defective LGs (see Table S1 in the supplementary material).

To characterize further the embryonic eyelid fusion defect, we performed histological analysis of eyelids from *Barx2*$^{+/+}$ and *Barx2*$^{-/-}$ E16.5 embryos. In *Barx2*$^{+/+}$ embryos, the edges of the top and bottom eyelids extended towards each other and fused, whereas *Barx2*$^{-/-}$ embryos had impaired or delayed extension. In those *Barx2*$^{-/-}$ embryos in which full eyelid extension did occur by E16.5, we still observed eyelid fusion delay (compare Fig. 2I and 2J). Surprisingly, the eyelid epithelial sheets of *Barx2*$^{+/+}$, *Barx2*$^{+/-}$ and *Barx2*$^{-/-}$ embryos showed no statistical difference in the number of cells positive for the proliferating cell markers Ki67 or PCNA (Fig. 2I-L). This suggests that failure of fusion relates to cell migration rather than proliferation defects. There was also no significant difference in the number of apoptotic cells in *Barx2*$^{-/-}$ eyelids compared with *Barx2*$^{+/+}$ eyelids (not shown). However, *Barx2*$^{-/-}$ eyelids appeared thinner than eyelids of wild-type and *Barx2*$^{+/-}$ littermates (Fig. 2I,J).

Barx2$^{-/-}$ mice have severe LG defects

LG development in mice starts at ~E13-13.5 as an invagination of the dorsal region of conjunctival epithelium (Makarenkova et al., 2000). This formation of a primary LG bud was strongly delayed

in *Barx2*$^{-/-}$ mice. At E15.0, the LG bud in *Barx2*$^{+/-}$ (Fig. 3A) and wild-type embryos (not shown) had already invaded the mesenchymal sac; by contrast, the LG bud in *Barx2*$^{-/-}$ embryos was either absent or much shorter (Fig. 3B-D). At E19-20, when LGs of *Barx2*$^{+/-}$ mice had extensively branched exorbital and intraorbital lobes (Fig. 3E), *Barx2*$^{-/-}$ LGs were generally vestigial and poorly branched (Fig. 3F-H). An important observation was that in addition to poor development of the distal lobes, *Barx2*$^{-/-}$ LGs often had ectopic budding from the proximal region of the LG duct (Fig. 3H). At postnatal day 4 (P4), *Barx2*$^{+/-}$ LGs were highly ramified whereas *Barx2*$^{-/-}$ LGs remained poorly branched, vestigial or, in some cases, absent (Fig. 3I-L).

Because there was substantial variation in *Barx2*$^{-/-}$ LG phenotypes between individual mice, we performed statistical analysis of LG development in twelve litters of E19.0 embryos. The *Barx2*$^{-/-}$ LG phenotype varied from almost normal to completely absent: relative to wild type, 64% of *Barx2*$^{-/-}$ LGs were smaller and substantially less branched, 18% of LGs were vestigial, and LGs were absent in 9% of mice. Only 9% of *Barx2*$^{-/-}$ mice had LGs that appeared morphologically normal or close to normal (slightly smaller). Overall, ~91% (P<0.001) of *Barx2*$^{-/-}$ LGs had defects in elongation of the primary duct and poor branching (Fig. 3M). These data indicate that Barx2 is important regulator of LG morphogenesis.

Antisense inhibition of Barx2 function alters LG branching

To confirm that the LG defects found in the *Barx2*$^{-/-}$ mouse are specific to loss of Barx2 function, we used *Barx2* antisense morpholino oligodeoxynucleotides (ODNs) to block *Barx2* expression in wild-type LGs (Meech et al., 2005). Whole LGs (organoids) containing only one bud (E15.5) (Fig. 4A) were explanted and cultured in serum-free medium. Antisense and control ODNs (sense and mismatched) were applied in Pluronic gel and uptake was monitored as described previously (Becker et al., 1999; Makarenkova and Patel, 1999; Makarenkova et al., 2000). *Barx2* antisense ODNs significantly affected LG morphogenesis (Fig. 4A): LGs cultured for 48 hours with *Barx2* antisense ODNs showed fewer (Fig. 4B) and shorter (Fig. 4C) branches than explants treated with control ODNs. These experiments confirm that Barx2 has an important role in LG branch elongation.

Barx2 is necessary for HG development

The primary HG bud invaginates from the nasal part of the conjunctival epithelium at E16.0 (Makarenkova et al., 2000). To determine whether lack of Barx2 affects HG development, whole-mount preparations of HG sacs from *Barx2*$^{+/+}$ and *Barx2*$^{-/-}$ embryos were stained with Hematoxylin and Eosin (Fig. 5A-F). *Barx2*$^{+/-}$ and *Barx2*$^{-/-}$ HGs were also studied in paraffin sections (Fig. 5G-J). In 99% of Barx2$^{-/-}$ HGs examined (112 glands; P<0.01), the epithelial component was absent (Fig. 5D-F,I-J). By contrast, development of the nasal gland, which does not express Barx2, was not altered in *Barx2*$^{-/-}$ mice relative to *Barx2*$^{+/-}$ mice (Fig. 5G,J, white arrowheads). These data suggest that Barx2 is necessary for HG development.

Barx2$^{-/-}$ mice show defects in MG patterning

MG placodes start to develop at E18.5 within the fused eyelid margin epithelium (Nien et al., 2010). At P3.5, we observed prominent epidermal tubular-like invaginations in wild-type eyelids (see arrowheads in Fig. S1A in the supplementary material),

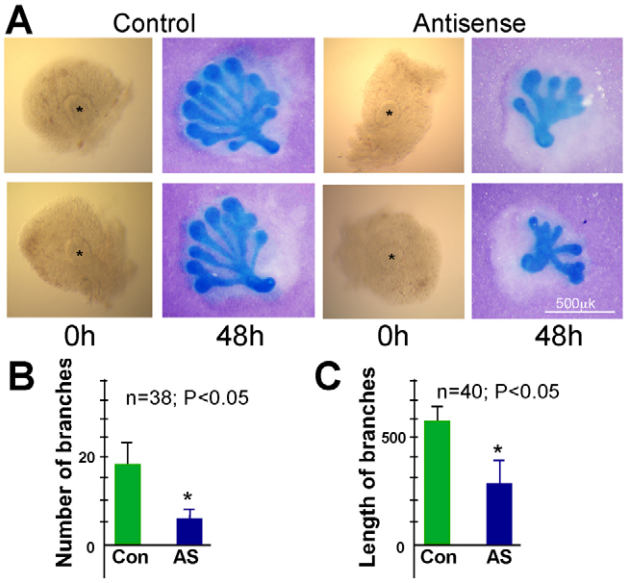

Fig. 4. Barx2 controls lacrimal gland (LG) branching morphogenesis ex vivo. (**A**) Application of antisense *Barx2* morpholino oligodeoxynucleotides (ODNs) to intact LGs isolated from Pax6 5.0-*lacZ* mice, suppresses branching by 48 hours whereas control scrambled ODNs do not. Epithelium is stained blue with X-gal. Asterisks indicate end bud. (**B**,**C**) Quantification of the number (B) and length (C) of branches after antisense ODN treatment. *n*, number of glands. Three independent experiments were performed. Error bars represent s.d. **P*<0.05.

whereas in *Barx2*$^{-/-}$ littermates these invaginations were much smaller (see arrowheads in Fig. S1B in the supplementary material). We also noticed that MGs in *Barx2*$^{-/-}$ mice often had an irregular spacing (compare Fig. 1K with Fig. 5K). At P8-10, MGs in wild-type eyelids had distinct acinar regions, whereas in *Barx2*$^{-/-}$ eyelids the acinar regions were poorly developed and variable in size and shape (see Fig. S1 in the supplementary material; compare Fig. S1C with S1F; S1D with S1E; and S1G with S1H). In adults (7 months of age), whole-mount preparations of wild-type upper eyelids showed MGs with a regular pattern and well-developed acinar regions (Fig. 5L), By contrast, MGs in adult *Barx2*$^{-/-}$ mice were generally smaller and often had an irregular size, shape and/or spacing, suggesting a role for Barx2 in MG morphogenesis and aging (Fig. 5M, arrowheads).

Barx2 regulates cell matrix and adhesion molecules during LG development

We found previously that Barx2 regulates cell adhesion and matrix remodeling (Meech et al., 2005; Stevens and Meech, 2006). Cell adhesion and cell-matrix interactions are crucial during branching morphogenesis of LGs and other ocular glands. We used a PCR-array focused on extracellular matrix (ECM) and adhesion molecules (SABiosciences, Qiagen) to compare gene expression in *Barx2*$^{-/-}$ and wild-type LGs at E18.0. Eleven out of 88 genes showed a greater than twofold decrease in expression in *Barx2*$^{-/-}$ glands relative to wild-type glands (Table 1). These genes included cadherins, integrin, laminins and matrix metalloproteinase 2 (Mmp2). The latter result is consistent with our previous findings that Barx2 regulates MMP and tissue inhibitors of metalloproteinases (TIMP) genes (Stevens et al., 2004; Stevens and Meech, 2006).

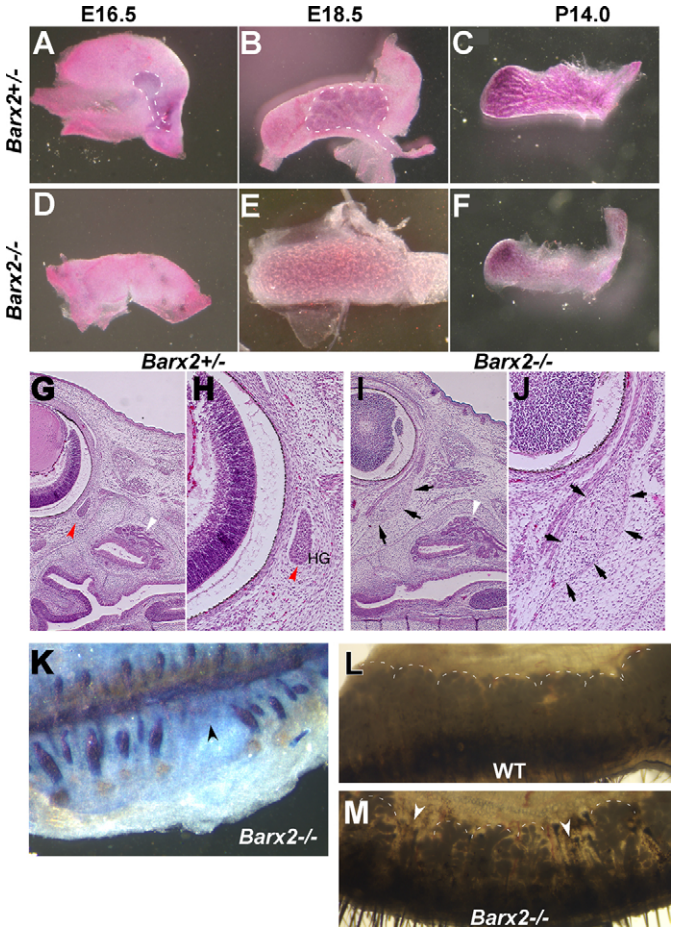

Fig. 5. Harderian gland (HG) and meibomian gland (MG) phenotypes in *Barx2* null mice. (**A-F**) Intact HGs isolated from *Barx2*$^{+/-}$ and *Barx2*$^{-/-}$ mice at different stages of development were stained with Hematoxylin. HG epithelium (dashed line) was present in *Barx2*$^{+/-}$ mice (A-C), but absent in *Barx2*$^{-/-}$ mice (D-F). (**G-J**) Sections of the ocular region from *Barx2*$^{+/-}$ and *Barx2*$^{-/-}$ embryos stained with Hematoxylin and Eosin. The primary Harderian bud (red arrowheads) can be identified in *Barx2*$^{+/-}$ embryos (G,H) but is absent in *Barx2*$^{-/-}$ embryos (I,J), although the mesenchyme remains (black arrows). The nasal gland is not affected in *Barx2*$^{-/-}$ mice (white arrowheads in G and I). (**K**) At P3.5, MGs of *Barx2*$^{-/-}$ mice have an irregular pattern (arrowhead; compare with Fig. 1K). (**L**,**M**) MGs in seven-month-old wild-type (L) and *Barx2*$^{-/-}$ (M) mice. MGs are outlined with a dashed line. In Barx2$^{-/-}$ mice, irregular MGs (missing or reduced glands) are indicated by arrowheads.

Barx2 regulates MMP expression and migration of the cells through ECM

Mmp2, Mmp9 and Mmp3 and various TIMPs have important roles in the development and normal function of branching organs (Giannelli et al., 1999; Joshi et al., 2006; Lelongt et al., 1997; Pohl et al., 2000; Simian et al., 2001; Zylberberg et al., 2007). To assess MMP and TIMP expression in the epithelium and mesenchyme of the LG, we performed RT-PCR for Timp1, Timp2, Timp3, Timp4, Mmp2, Mmp3 and Mmp9 on isolated epithelial and mesenchymal LG components (see Table S2 in the supplementary material). Barx1 (expressed in mesenchyme) and Barx2 (expressed in epithelium) expression was used as a reference to ensure complete separation of epithelium and mesenchyme. Timp1, Timp2, Mmp2 and Mmp9 were expressed in both epithelial and mesenchymal components of the gland, whereas Timp3, Timp4 and Mmp3 were expressed only in the mesenchyme (see Table S2 in the supplementary material). Immunostaining of LGs at E16.5-17.0 with Mmp2, Mmp3 and Mmp9 antibodies confirmed that Mmp2 and Mmp9 were expressed in both epithelium and mesenchyme (Fig. 6A), whereas Mmp3 was expressed only in mesenchyme (not shown).

Table 1. Changes in gene expression in *Barx2*$^{-/-}$ lacrimal glands (LGs)

Gene	Fold change	*P* value
Cdh3	–5.6623	=0.04
Cdh4	–3.231	<0.01
Vcan	–6.2844	<0.05
Ctgf	–2.9968	<0.05
Itga5	–3.9145	<0.04
Lama2	–7.212	<0.05
Lamb2	–2.4102	<0.001
Mmp2	–6.3216	<0.001
Sgce	–6.928	<0.05
Sparc	–9.5803	<0.05
Tnc	–2.7239	<0.05

Results of three independent experiments comparing *Barx2*$^{-/-}$ and wild-type LGs in RT-PCR arrays. Genes encoding the matrix metallopeptidase Mmp2; the cell adhesion molecules cadherins 3 and 4 (Cdh3 and Cdh4) and tenascin C (Tnc); integrin alpha 5 (Itga5); the cell matrix molecules laminin alpha 2 and laminin beta 2 (Lama2, Lamb2) and sarcoglycan (Sgce); and secreted acidic cysteine rich glycoprotein (Sparc) are downregulated by at least twofold (P<0.05) in *Barx2*$^{-/-}$ LGs at E17.5 relative to wild-type LGs.

LG bud elongation requires remodeling of the ECM around the bud tip by matrix remodeling enzymes including MMPs (Ganser et al., 1991; Hinck and Silberstein, 2005). Thus, reduced expression of MMPs in the *Barx2*$^{-/-}$ LG might affect bud propagation, resulting in impairment of both extension and branching as seen in Fig. 3. To determine whether Barx2 controls MMP production, culture media from explanted Barx2$^{-/-}$ and wild-type LG epithelial buds were analyzed by gelatin zymography. Barx2$^{-/-}$ buds showed decreased MMP secretion compared with wild-type buds (Fig. 6B). The expression of several MMPs and TIMPs was also compared in whole LG from E19.5 *Barx2*$^{-/-}$ and wild-type embryos by RT-PCR. Expression of Mmp9 and Mmp3 was greatly reduced in Barx2$^{-/-}$ LGs, Mmp2 and Timp1 expression was slightly reduced and Barx1 expression was unchanged (see Fig. S2 in the supplementary material).

We next performed a gain-of-function experiment by transiently transfecting A253 epithelial cells with either pcDNA3-Barx2 expression plasmid or empty pcDNA3 plasmid. Overexpression of Barx2 increased both Mmp2 and Mmp9 secretion (Fig. 6C). To determine whether overexpression of Barx2 altered epithelial migration, we used a transwell cell migration assay. A253 cells transfected with either pcDNA3-Barx2 or pcDNA3 were seeded onto 2 mg/ml Matrigel in the upper chamber of the transwell (Fig. 6D). Fibronectin was used as the chemoattractant in the lower chamber. After 24 hours, cells that had migrated through the polycarbonate membrane were stained. Barx2 overexpression induced more rapid migration through the Matrigel relative to control-transfected cells (Fig. 6E). We also observed that Barx2-transfected A253 cells embedded in Matrigel formed tubular structures, whereas control transfected cells did not (Fig. 6F). We have reported similar effects of Barx2 overexpression in mammary epithelial cells (Stevens and Meech, 2006). This suggests a role for Barx2 in driving complex epithelial cell organization, probably via regulated cell adhesion and MMP-dependent ECM remodeling.

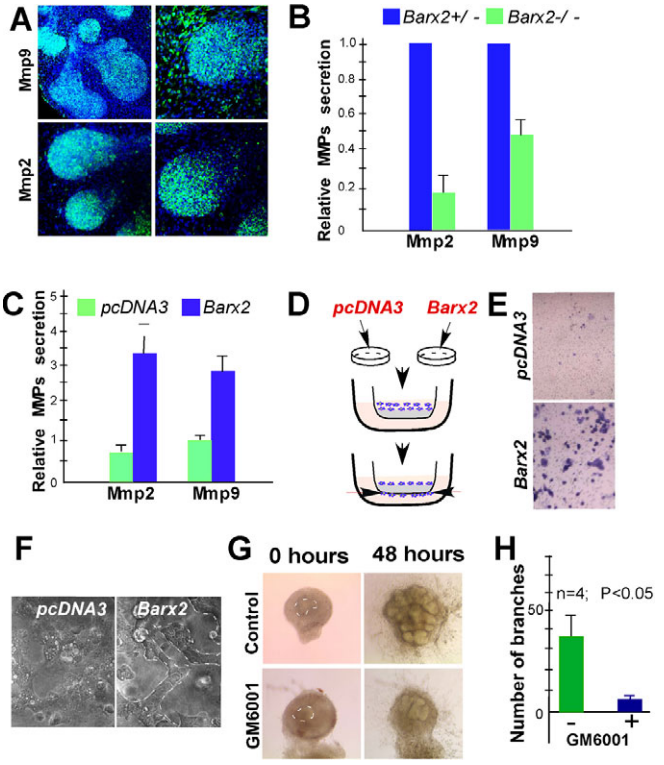

Fig. 6. Barx2 regulates matrix metalloproteinase (MMP) expression in lacrimal glands (LGs) and epithelial cells. (**A**) Immunostaining of LGs at E16 with Mmp2 and Mmp9 antibodies (green) shows that Mmp2 is mostly expressed in the epithelium, whereas Mmp9 is expressed in both epithelium and mesenchyme. Nuclei are stained with DAPI (blue). (**B**) MMP secretion is reduced in Barx2$^{-/-}$ LGs. Graph of gelatin zymography assay measuring Mmp2 and Mmp9 in conditioned media from wild-type and Barx2$^{-/-}$ epithelial explants cultured in serum-reduced Matrigel. (**C**) Barx2 overexpression increases secretion of MMPs in A253 cells. Graph of gelatin zymography assay measuring Mmp2 or Mmp9 in conditioned media from transfected A253 cells cultured in wells coated with Matrigel. (**D**,**E**) Barx2 increases cell migration. (D) Schematic of the Transwell migration assay. (E) A253 epithelial cells transfected with either the pcDNA3-Barx2 vector or empty pcDNA3 vector were plated onto Transwell filters coated with Matrigel. Fibronectin was added to the media below the inserts as a chemical attractant. After 24 hours, migrated cells were stained with Cresyl Violet. Barx2 overexpression induces rapid migration of A253 cells. (**F**) Barx2 overexpression increases aggregation and promotes formation of tubular structures (dashed line) by A253 cells grown in Matrigel. (**G**) The MMP inhibitor GM6001 retards branching of whole LG explants. Dashed lines encircle end bud. (**H**) Quantification of secondary buds and branches formed by control-treated (n=4; 38 glands) and GM 6001-treated (n=4; 37glands) whole E15.5 LG buds after 48 hours of culture. P<0.05 (Student's t-test). For all graphs, error bars represent s.d.

To determine whether MMPs are required for LG budding and branching in ex vivo culture, we used GM6001, which inhibits multiple MMPs in vivo (Wiseman et al., 2003). Wild-type intact E16.0 LG organoids were treated with GM6001 or DMSO vehicle. Vehicle-treated LG organoids formed buds and extended branches through the mesenchyme and ECM (Fig. 6G). GM6001 inhibited bud extension and branching (Fig. 6G,H); this result was very similar to the effect of Barx2-antisense treatment (Fig. 4). Thus, bud elongation and branching requires MMP activity.

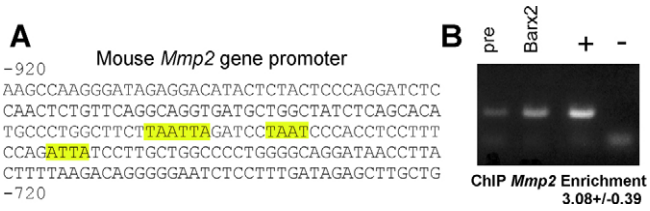

Fig. 7. Chromatin immunoprecipitation (ChIP) analysis of Barx2 binding to the mouse *Mmp2* promoter in E17.5-18.0 lacrimal glands (LGs). (**A**,**B**) ChIP was performed using Barx2 antibodies (Santa Cruz) or preimmune (pre) serum and the region of the *Mmp2* gene promoter containing predicted Barx2 binding sites (highlighted in A) was amplified by PCR.

Barx2 binds to the *Mmp2* gene

We performed multi-species sequence alignment to identify potential Barx2 binding sites within *Mmp2* and *Mmp9* promoters. Clusters of sequences corresponding to core homeobox binding site (HBS) motifs (ATTA) were identified at approximately –830 bp upstream of the predicted transcription start site (TSS) in the mouse and rat Mmp2 promoters and –900bp in the human promoter (see Fig. S3 in the supplementary material, Fig. 7A). Previous work suggests that clustered ATTA motifs favor Barx2 binding (Stevens et al., 2004). Clustered HBS motifs were also found within the human *MMP9* promoter at approximately –890 bp; however, there was no comparable sequence within the mouse and rat promoters.

Barx2 binding to the *Mmp2* promoter was examined by chromatin immunoprecipitation (ChIP) in wild-type mouse LGs using rabbit anti-Barx2 antibody (Santa Cruz) as previously described (Stevens et al., 2004). Enrichment of the region containing the HBS motifs was assessed by PCR and gel densitometry (Fig. 7B). There was a threefold enrichment of the target region suggesting that Barx2 can directly regulate *Mmp2*.

Barx2 regulates LG branching response to Fgf10

We showed previously that Fgf10 is a key regulator of LG branching morphogenesis (Makarenkova et al., 2009). To determine whether there is a functional interaction between Fgf10 and Barx2 in LG development, we examined the effect of Barx2 on Fgf10-induced LG bud migration. LG epithelial buds isolated from E15.5 *Barx2*$^{-/-}$ and *Barx2*$^{+/-}$ embryos were plated in Matrigel and exposed to a local diffusible source of Fgf10 via Fgf10-soaked heparin acrylic beads placed 0.1 mm from the distal tip of the buds (Makarenkova et al., 2009; Weaver et al., 2000). Bud growth was monitored over 24-72 hours. *Barx2*$^{+/-}$ buds elongated towards the Fgf10 beads and majority of them made contact with the bead within 36 hours (Fig. 8A,C). By contrast, *Barx2*$^{-/-}$ buds did not elongate towards the bead and did not make contact within this time (Fig. 8B,C). This suggests a requirement for Barx2 in receiving or transducing FGF signals. To assess the relative roles of Barx2 and Fgf10 in the regulation of MMPs, we measured Mmp2 and Mmp9 secretion in pcDNA3-Barx2 and control pcDNA3 transfected A253 cells with or without Fgf10 stimulation (Fig. 8D). Both overexpression of Barx2 and Fgf10 treatment increased MMP secretion; however, the effect of both treatments was additive (Fig. 8D). Overall, it is likely that Fgf10 and Barx2 are both required to generate an optimal level of MMP secretion for matrix remodeling and epithelial bud elongation.

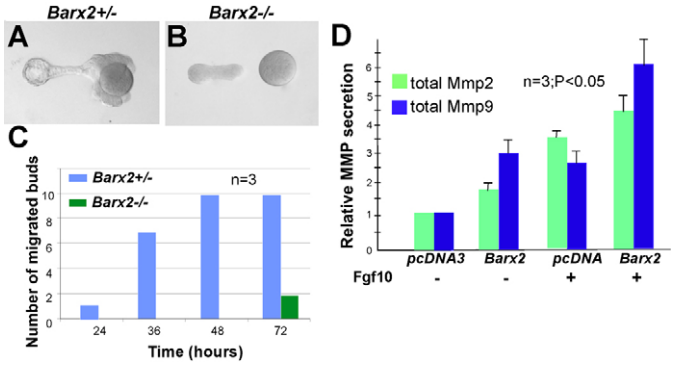

Fig. 8. Barx2 and Fgf10 regulate lacrimal gland (LG) bud migration and Mmp2 and Mmp9 expression. (**A-C**) LG ex vivo migration assay (48 hours) was performed using LG buds explanted from E15.5 Barx2$^{+/-}$ (A) and Barx2$^{-/-}$ (B) embryos. (C) Elongation towards an Fgf10-loaded bead was monitored for 24-72 hours. The number of explants of each genotype that made contact with the bead at four time points between 24 and 72 hours is plotted. *n*, number of experiments. (**D**) Barx2 and Fgf10 increase total Mmp2 and Mmp9 protein secretion as determined by zymography. A253 epithelial cells were transfected with pcDNA3-Barx2 expression vector or with pcDNA3 (control) and the expression of both MMPs was estimated in the presence (+) or absence (–) of Fgf10. Error bars represent s.d.

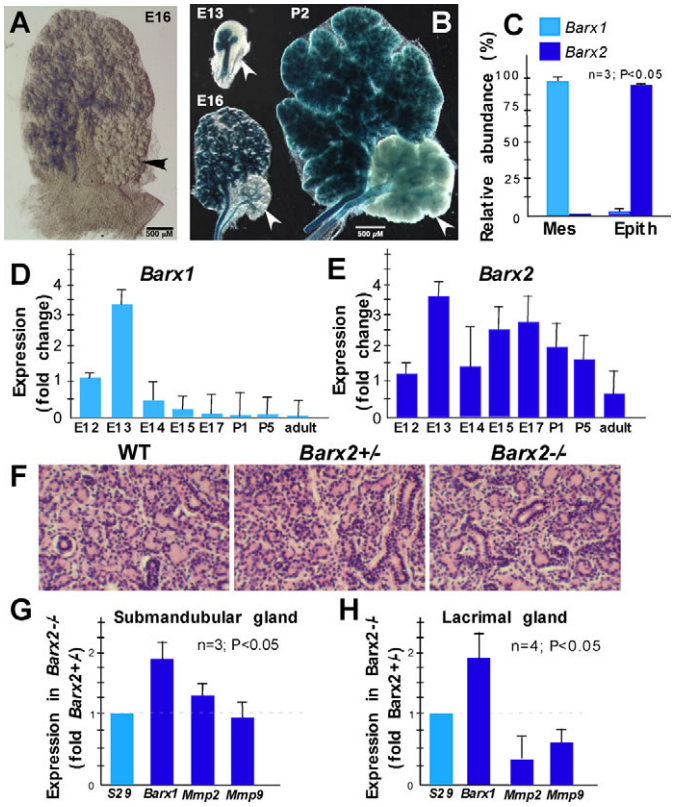

Fig. 9. *Barx* gene expression during submandibular gland (SMG) development. (**A**) In situ hybridization showing *Barx2* mRNA expression in the SMG and little or no expression in the sublingual gland. Arrowhead indicates sublingual gland. (**B**) *Barx2-lacZ*-driven β-galactosidase expression was detected in the epithelial component of SMGs at E13, E16 and P2 whereas the sublingual gland had less expression. Arrowheads indicate sublingual gland. (**C**) Quantitative RT-PCR analysis of isolated epithelial and mesenchymal components of the E13 SMG. *Barx1* is expressed in the mesenchyme and *Barx2* is expressed in the epithelium. (**D**,**E**) Quantitative RT-PCR analysis of *Barx1* (D) and *Barx2* (E) expression relative to the E12 stage and normalized to *Rps29* in SMGs throughout embryonic and postnatal development and in the adult mouse. *Barx1* is expressed early in SMG formation (E12-13) whereas *Barx2* remains expressed throughout SMG morphogenesis and maturation. (**F**) Hematoxylin and Eosin staining of P4 SMG shows no difference between wild-type (WT), Barx2$^{+/-}$ and Barx2$^{-/-}$ SMGs. (**G**,**H**) Real-time RT-PCR analysis of Barx and MMP gene expression in E13 SMG (G) and E17 LG (H) normalized to S29 and presented as fold change in expression in Barx2$^{-/-}$ relative to Barx2$^{+/-}$ mice. Expression of *Mmp2* and *Mmp9* genes are downregulated in Barx2$^{-/-}$ LGs, but not in SMGs. *Barx1* is slightly elevated in Barx2$^{-/-}$ LGs and SMGs. For all graphs, error bars represent s.d.

Barx2 expression in salivary glands

In situ hybridization and β-galactosidase staining of salivary glands isolated from *Barx2*$^{+/-}$ mice showed that Barx2 was strongly expressed throughout the epithelial component of the submandibular gland (SMG) (Fig. 9A,B), as well as in parotid glands (not shown). By contrast, Barx2 expression in sublingual glands was low (Fig. 9A,B). Similar to ocular glands, Barx2 is expressed only in the SMG epithelium, whereas Barx1 expression was restricted to the mesenchyme (Fig. 9C). The level of Barx1 expression was highest at the early stages of SMG development (E13), whereas Barx2 expression was relatively high during all stages of SMG development (Fig. 9D,E). We next analyzed *Barx2*$^{-/-}$ mice for defects in SMG development. Surprisingly, *Barx2*$^{-/-}$ SMGs were a normal size and branching appeared normal histologically (Fig. 9F). The levels of *Mmp2* and *Mmp9* in *Barx2*$^{-/-}$ SMG as determined by quantitative RT-PCR (qRT-PCR) were unchanged relative to *Barx2*$^{+/-}$ SMG (Fig. 9G,H). Thus, it appears that Barx2, whilst important for ocular gland development, might be redundant in the SMG.

DISCUSSION

A considerable body of evidence indicates that branching morphogenesis is dependent on the ECM, ECM-receptors such as integrins, and ECM-remodeling enzymes such as MMPs and TIMPs. In this study, we showed that Barx2 is important for LG and MG morphogenesis and for normal eyelid fusion. Moreover, Barx2 is essential for HG formation. Importantly, the chemotactic response of LG epithelium to Fgf10 was inhibited by loss of Barx2, suggesting that Barx2 mediates epithelial responses to FGFs during branching morphogenesis. In addition, we determined that both Barx2 and Fgf10 control expression of MMPs. Together, these factors might provide dynamic regulation of cell-matrix interactions facilitating epithelial bud elongation and branching.

Barx2 is an important regulator of matrix remodeling and morphogenesis of ocular glands

Matrix remodeling by MMPs has been demonstrated during branching morphogenesis of lung (Gill et al., 2003; Parks and Shapiro, 2001), salivary glands (Oblander et al., 2005; Rebustini et al., 2009), kidney (Meyer et al., 2004) and mammary glands (Kouros-Mehr and Werb, 2006). The regulation of MMP expression and the role of MMPs in regulation of LG branching morphogenesis are not as well studied. However, the balance of MMP expression is known to be important for adult LG epithelial cell survival (Zylberberg et al., 2007). For example, Mmp3 and

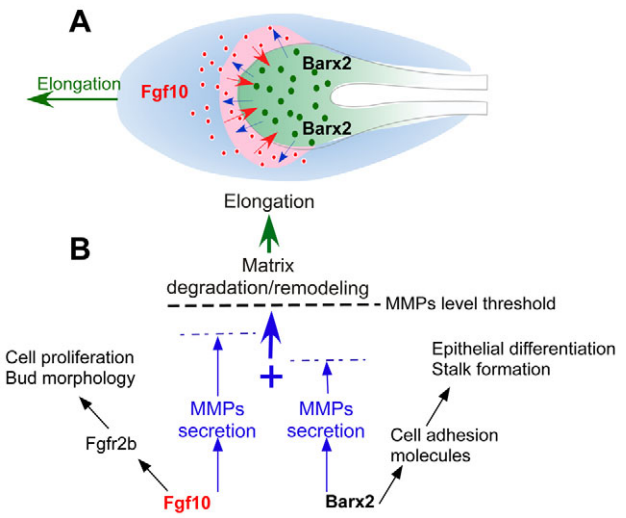

Fig. 10. Model of Barx2 and FGF signaling in pericellular extracellular matrix (ECM) remodeling during lacrimal gland (LG) bud morphogenesis. (**A**) Fgf10 (pink) is expressed in the mesenchyme (blue) and it is a chemical attractant for epithelial cells (green). Fgf10 binds Fgfr2b and signals intracellularly (red arrows) to induce cell proliferation (green circles) and positively regulate matrix metalloproteinase (MMP) secretion (blue arrows), which digest extracellular matrix (red circles), thus promoting migration. Barx2 expressed in the epithelium renders the epithelial cells competent to respond chemotactically to FGF signals, in part by either cooperative or parallel induction of MMPs. (**B**) Bud elongation might require a critical threshold level of MMPs. The combined effect of Barx2 and FGF on MMP expression induces efficient matrix remodeling and rapid LG bud elongation. Blue dashed lines represent the intermediate levels of MMPs.

Mmp9 are increased in the LGs of patients suffering from the autoimmune disease Sjögren's syndrome, which correlates with the severity of the disease (Solomon et al., 2001). Thus, precise regulation of MMPs is likely to be crucial for LG development, maintenance and function; overproduction of MMPs might lead to glandular destruction (Ram et al., 2006).

Development of the LG depends upon interactions between epithelium, surrounding mesenchyme, and ECM (Govindarajan et al., 2000; Makarenkova et al., 2000). Loss of Barx2 leads to strongly reduced or vestigial LGs and over-expression of Barx2 in A253 cells accelerates their migration and aggregation into tubular structures in Matrigel. Together these data suggest that Barx2 controls branching and budding through interactions of epithelial cells with the ECM. Moreover, given that Mmp2 and Mmp9 expression were downregulated in *Barx2*$^{-/-}$ LG and that MMP inhibition blocked bud elongation and branching, it is likely that Barx2 functions via MMPs to control propagation of the lacrimal bud through the mesenchymal matrix.

Cooperation of Barx2 and FGF signaling in branching morphogenesis

Recent studies have broadened the function of MMPs beyond mechanical remodeling of the ECM to include modulation of cell proliferation through activation or inhibition of signaling molecules, such as growth factors and their receptors. Degradation of ECM by MMPs can release FGFs and FGF-binding HS from proteoglycans and might regulate the shape of FGF gradients and, hence, the spatiotemporal domain of cell proliferation (Makarenkova et al., 2009; Patel et al., 2007; Patel et al., 2006). Moreover, it has been shown that during SMG branching morphogenesis MMPs can regulate FGF signaling by direct cleavage of FGF receptors (FGFRs) (Levi et al., 1996).

The observation that Barx2$^{-/-}$ LG buds showed impaired chemotaxis towards Fgf10-soaked beads indicates that Barx2 transduces FGF signals. This might involve direct regulation of FGFRs in the epithelial cells of the invading bud, or alteration of MMP secretion by the bud, which in turn can modulate the release of ECM-bound FGFs and the activity of cell surface FGFRs. However, further studies are required to uncover the precise roles and functional interactions of Barx2, FGFs and ECM remodeling in branching morphogenesis.

Overall, the data presented here suggest that a general mechanism of Barx2 action in branching morphogenesis might be regulation of matrix remodeling by MMPs. This could affect epithelial cell-matrix interactions both by degrading ECM ahead of the invading epithelial bud and by modulating the signaling mediated by growth factors such as FGFs (Fig. 10). Barx2 is also likely to influence epithelial cell aggregation via regulation of cell adhesion molecule expression.

Barx2 is necessary for HG development

We found that Barx2 was expressed in the epithelial component of the HG, and that HG epithelia are absent in almost all *Barx2*$^{-/-}$ mice, with a few showing an epithelial rudiment. Thus, Barx2 is essential for HG development. *Barx2* null mice present an interesting opportunity to assess the importance of the HG in protecting the eye. Although all *Barx2*$^{-/-}$ mice lacked functional HGs, only a small proportion developed ocular surface damage and this was more likely to be related to early eyelid fusion defects or reduced lubrication by the diminished LGs and MGs. Thus, the HG might have a largely redundant function in lubricating the ocular surfaces and protecting against eyelid friction and desiccation; other suggested functions for HGs include photoprotection and immune response.

Barx2 is a specific regulator of ocular glands development

Given the dramatic effects of loss of Barx2 on LG, MG and HG development, it is interesting that SMGs, which also express Barx2, are normal in *Barx2* null mice. Moreover, other branching organs (such as lung and prostate) in which Barx2 expression has been reported previously (Jones et al., 1997) were also normal in *Barx2* null mice (our unpublished observations). This might be due to compensation by other factors, including other homeobox factors that can regulate MMP expression or secretion.

Taken together, our data suggest that Barx2 is a specific regulator of ocular gland development. As well as providing a fundamental understanding of the morphogenetic pathways underlying the development of ocular glands, the study of Barx2 and its regulation of MMPs might give new insights into pathogenic processes in Sjögren's syndrome and other forms of dry eye disease.

Acknowledgements

H.P.M. was supported by a National Eye Institute at National Institutes of Health Grant 1 R21 EY021292-01, by the Neurosciences Research Foundation and by the Sjögren's Syndrome Foundation; M.I. was supported by a grant from National Defense Medical College (Japan); M.P.H. was supported by the Intramural Research Program of the National Institute for Dental and Craniofacial Research at the National Institutes of Health. Deposited in PMC for release after 12 months.

Competing interests statement
The authors declare no competing financial interests.

Supplementary material
Supplementary material for this article is available at
http://dev.biologists.org/lookup/suppl/doi:10.1242/dev.066241/-/DC1

References

Ahrens, K. and Schlosser, G. (2005). Tissues and signals involved in the induction of placodal Six1 expression in Xenopus laevis. *Dev. Biol.* **288**, 40-59.
Becker, D. L., McGonnell, I., Makarenkova, H. P., Patel, K., Tickle, C., Lorimer, J. and Green, C. R. (1999). Roles for alpha 1 connexin in morphogenesis of chick embryos revealed using a novel antisense approach. *Dev. Genet.* **24**, 33-42.
Chen, B., Kim, E. H. and Xu, P. X. (2009). Initiation of olfactory placode development and neurogenesis is blocked in mice lacking both Six1 and Six4. *Dev. Biol.* **326**, 75-85.
Dean, C., Ito, M., Makarenkova, H. P., Faber, S. C. and Lang, R. A. (2004). Bmp7 regulates branching morphogenesis of the lacrimal gland by promoting mesenchymal proliferation and condensation. *Development* **131**, 4155-4165.
Dudley, A. T., Godin, R. E. and Robertson, E. J. (1999). Interaction between FGF and BMP signaling pathways regulates development of metanephric mesenchyme. *Genes Dev.* **13**, 1601-1613.
Faber, S. C., Robinson, M. L., Makarenkova, H. P. and Lang, R. A. (2002). Bmp signaling is required for development of primary lens fiber cells. *Development* **129**, 3727-3737.
Franklin, R. M. (1989). The ocular secretory immune system: a review. *Curr. Eye Res.* **8**, 599-606.
Galardy, R. E., Cassabonne, M. E., Giese, C., Gilbert, J. H., Lapierre, F., Lopez, H., Schaefer, M. E., Stack, R., Sullivan, M., Summers, B. et al. (1994a). Low molecular weight inhibitors in corneal ulceration. *Ann. N. Y. Acad. Sci.* **732**, 315-323.
Galardy, R. E., Grobelny, D., Foellmer, H. G. and Fernandez, L. A. (1994b). Inhibition of angiogenesis by the matrix metalloprotease inhibitor N-[2R-2-(hydroxamidocarbonymethyl)-4-methylpentanoyl)]-L-tryptophan methylamide. *Cancer Res.* **54**, 4715-4718.
Ganser, G. L., Stricklin, G. P. and Matrisian, L. M. (1991). EGF and TGF alpha influence in vitro lung development by the induction of matrix-degrading metalloproteinases. *Int. J. Dev. Biol.* **35**, 453-461.
Giannelli, G., Pozzi, A., Stetler-Stevenson, W. G., Gardner, H. A. and Quaranta, V. (1999). Expression of matrix metalloprotease-2-cleaved laminin-5 in breast remodeling stimulated by sex steroids. *Am. J. Pathol.* **154**, 1193-1201.
Gijbels, K., Galardy, R. E. and Steinman, L. (1994). Reversal of experimental autoimmune encephalomyelitis with a hydroxamate inhibitor of matrix metalloproteases. *J. Clin. Invest.* **94**, 2177-2182.
Gill, S. E., Pape, M. C., Khokha, R., Watson, A. J. and Leco, K. J. (2003). A null mutation for tissue inhibitor of metalloproteinases-3 (Timp-3) impairs murine bronchiole branching morphogenesis. *Dev. Biol.* **261**, 313-323.
Govindarajan, V., Ito, M., Makarenkova, H. P., Lang, R. A. and Overbeek, P. A. (2000). Endogenous and ectopic gland induction by FGF-10. *Dev. Biol.* **225**, 188-200.
Grobelny, D., Poncz, L. and Galardy, R. E. (1992). Inhibition of human skin fibroblast collagenase, thermolysin, and Pseudomonas aeruginosa elastase by peptide hydroxamic acids. *Biochemistry* **31**, 7152-7154.
Herring, B. P., Kriegel, A. M. and Hoggatt, A. M. (2001). Identification of Barx2b, a serum response factor-associated homeodomain protein. *J. Biol. Chem.* **276**, 14482-14489.
Hinck, L. and Silberstein, G. B. (2005). Key stages in mammary gland development: the mammary end bud as a motile organ. *Breast Cancer Res.* **7**, 245-251.
Hogan, B. L., Grindley, J., Bellusci, S., Dunn, N. R., Emoto, H. and Itoh, N. (1997). Branching morphogenesis of the lung: new models for a classical problem. *Cold Spring Harb. Symp. Quant. Biol.* **62**, 249-256.
Jones, F. S., Kioussi, C., Copertino, D. W., Kallunki, P., Holst, B. D. and Edelman, G. M. (1997). Barx2, a new homeobox gene of the Bar class, is expressed in neural and craniofacial structures during development. *Proc. Natl. Acad. Sci. USA* **94**, 2632-2637.
Joshi, P. A., Chang, H. and Hamel, P. A. (2006). Loss of Alx4, a stromally-restricted homeodomain protein, impairs mammary epithelial morphogenesis. *Dev. Biol.* **297**, 284-294.
Knop, E., Knop, N., Millar, T., Obata, H. and Sullivan, D. A. (2011). The international workshop on meibomian gland dysfunction: report of the subcommittee on anatomy, physiology, and pathophysiology of the meibomian gland. *Invest. Ophthalmol. Vis. Sci.* **52**, 1938-1978.
Kouros-Mehr, H. and Werb, Z. (2006). Candidate regulators of mammary branching morphogenesis identified by genome-wide transcript analysis. *Dev. Dyn.* **235**, 3404-3412.
Laclef, C., Souil, E., Demignon, J. and Maire, P. (2003). Thymus, kidney and craniofacial abnormalities in Six 1 deficient mice. *Mech. Dev.* **120**, 669-679.
Lelongt, B., Trugnan, G., Murphy, G. and Ronco, P. M. (1997). Matrix metalloproteinases MMP2 and MMP9 are produced in early stages of kidney morphogenesis but only MMP9 is required for renal organogenesis in vitro. *J. Cell Biol.* **136**, 1363-1373.
Levi, E., Fridman, R., Miao, H. Q., Ma, Y. S., Yayon, A. and Vlodavsky, I. (1996). Matrix metalloproteinase 2 releases active soluble ectodomain of fibroblast growth factor receptor 1. *Proc. Natl. Acad. Sci. USA* **93**, 7069-7074.
Lu, P., Sternlicht, M. D. and Werb, Z. (2006). Comparative mechanisms of branching morphogenesis in diverse systems. *J. Mammary Gland Biol. Neoplasia* **11**, 213-228.
Makarenkova, H. and Patel, K. (1999). Gap junction signalling mediated through connexin-43 is required for chick limb development. *Dev. Biol.* **207**, 380-392.
Makarenkova, H. P., Ito, M., Govindarajan, V., Faber, S. C., Sun, L., McMahon, G., Overbeek, P. A. and Lang, R. A. (2000). FGF10 is an inducer and Pax6 a competence factor for lacrimal gland development. *Development* **127**, 2563-2572.
Makarenkova, H. P., Hoffman, M. P., Beenken, A., Eliseenkova, A. V., Meech, R., Tsau, C., Patel, V. N., Lang, R. A. and Mohammadi, M. (2009). Differential interactions of FGFs with heparan sulfate control gradient formation and branching morphogenesis. *Sci. Signal.* **2**, ra55.
Meech, R., Edelman, D. B., Jones, F. S. and Makarenkova, H. P. (2005). The homeobox transcription factor Barx2 regulates chondrogenesis during limb development. *Development* **132**, 2135-2146.
Metzger, R. J. and Krasnow, M. A. (1999). Genetic control of branching morphogenesis. *Science* **284**, 1635-1639.
Meyer, T. N., Schwesinger, C., Bush, K. T., Stuart, R. O., Rose, D. W., Shah, M. M., Vaughn, D. A., Steer, D. L. and Nigam, S. K. (2004). Spatiotemporal regulation of morphogenetic molecules during in vitro branching of the isolated ureteric bud: toward a model of branching through budding in the developing kidney. *Dev. Biol.* **275**, 44-67.
Monte, J. C., Sakurai, H., Bush, K. T. and Nigam, S. K. (2007). The developmental nephrome: systems biology in the developing kidney. *Curr. Opin. Nephrol. Hypertens.* **16**, 3-9.
Nien, C. J., Massei, S., Lin, G., Liu, H., Paugh, J. R., Liu, C. Y., Kao, W. W., Brown, D. J. and Jester, J. V. (2010). The development of meibomian glands in mice. *Mol. Vis.* **16**, 1132-1140.
Oblander, S. A., Zhou, Z., Galvez, B. G., Starcher, B., Shannon, J. M., Durbeej, M., Arroyo, A. G., Tryggvason, K. and Apte, S. S. (2005). Distinctive functions of membrane type 1 matrix-metalloprotease (MT1-MMP or MMP-14) in lung and submandibular gland development are independent of its role in pro-MMP-2 activation. *Dev. Biol.* **277**, 255-269.
Olson, L. E., Zhang, J., Taylor, H., Rose, D. W. and Rosenfeld, M. G. (2005). Barx2 functions through distinct corepressor classes to regulate hair follicle remodeling. *Proc. Natl. Acad. Sci. USA* **102**, 3708-3713.
Ostle, B. and Mensing, R. W. (1975). *Statistics in Research: Basic Concepts and Techniques for Research Workers*. Des Moines, IA: The Iowa University Press.
Pan, Y., Carbe, C., Powers, A., Zhang, E. E., Esko, J. D., Grobe, K., Feng, G. S. and Zhang, X. (2008). Bud specific N-sulfation of heparan sulfate regulates Shp2-dependent FGF signaling during lacrimal gland induction. *Development* **135**, 301-310.
Parks, W. C. and Shapiro, S. D. (2001). Matrix metalloproteinases in lung biology. *Respir. Res.* **2**, 10-19.
Patel, V. N., Rebustini, I. T. and Hoffman, M. P. (2006). Salivary gland branching morphogenesis. *Differentiation* **74**, 349-364.
Patel, V. N., Knox, S. M., Likar, K. M., Lathrop, C. A., Hossain, R., Eftekhari, S., Whitelock, J. M., Elkin, M., Vlodavsky, I. and Hoffman, M. P. (2007). Heparanase cleavage of perlecan heparan sulfate modulates FGF10 activity during ex vivo submandibular gland branching morphogenesis. *Development* **134**, 4177-4186.
Patel, V. N., Likar, K. M., Zisman-Rozen, S., Cowherd, S. N., Lassiter, K. S., Sher, I., Gallagher, J. T., Yates, E. A., Turnbull, J. E., Ron, D. et al. (2008). Specific heparan sulfate structures modulate FGF10-mediated submandibular gland epithelial morphogenesis and differentiation. *J. Biol. Chem.* **283**, 9308-9317.
Payne, A. P. (1994). The harderian gland: a tercentennial review. *J. Anat.* **185**, 1-49.
Pohl, M., Sakurai, H., Bush, K. T. and Nigam, S. K. (2000). Matrix metalloproteinases and their inhibitors regulate in vitro ureteric bud branching morphogenesis. *Am. J. Physiol. Renal Physiol.* **279**, F891-F900.
Ram, M., Sherer, Y. and Shoenfeld, Y. (2006). Matrix metalloproteinase-9 and autoimmune diseases. *J. Clin. Immunol.* **26**, 299-307.
Rebustini, I. T., Myers, C., Lassiter, K. S., Surmak, A., Szabova, L., Holmbeck, K., Pedchenko, V., Hudson, B. G. and Hoffman, M. P. (2009). MT2-MMP-dependent release of collagen IV NC1 domains regulates submandibular gland branching morphogenesis. *Dev. Cell* **17**, 482-493.
Sakai, T. (2009). Epithelial branching morphogenesis of salivary gland: exploration of new functional regulators. *J. Med. Invest.* **56 Suppl**, 234-238.

Sander, G., Bawden, C. S., Hynd, P. I., Nesci, A., Rogers, G. and Powell, B. C. (2000). Expression of the homeobox gene, Barx2, in wool follicle development. *J. Invest. Dermatol.* **115**, 753-756.

Satoh, Y., Gesase, A. P., Habara, Y., Ono, K. and Kanno, T. (1996). Lipid secretory mechanisms in the mammalian harderian gland. *Microsc. Res. Tech.* **34**, 104-110.

Sellar, G. C., Li, L., Watt, K. P., Nelkin, B. D., Rabiasz, G. J., Stronach, E. A., Miller, E. P., Porteous, D. J., Smyth, J. F. and Gabra, H. (2001). BARX2 induces cadherin 6 expression and is a functional suppressor of ovarian cancer progression. *Cancer Res.* **61**, 6977-6981.

Sellar, G. C., Watt, K. P., Li, L., Nelkin, B. D., Rabiasz, G. J., Porteous, D. J., Smyth, J. F. and Gabra, H. (2002). The homeobox gene BARX2 can modulate cisplatin sensitivity in human epithelial ovarian cancer. *Int. J. Oncol.* **21**, 929-933.

Simian, M., Hirai, Y., Navre, M., Werb, Z., Lochter, A. and Bissell, M. J. (2001). The interplay of matrix metalloproteinases, morphogens and growth factors is necessary for branching of mammary epithelial cells. *Development* **128**, 3117-3131.

Solomon, A., Dursun, D., Liu, Z., Xie, Y., Macri, A. and Pflugfelder, S. C. (2001). Pro- and anti-inflammatory forms of interleukin-1 in the tear fluid and conjunctiva of patients with dry-eye disease. *Invest. Ophthalmol. Vis. Sci.* **42**, 2283-2292.

Song, D. L., Chalepakis, G., Gruss, P. and Joyner, A. L. (1996). Two Pax-binding sites are required for early embryonic brain expression of an Engrailed-2 transgene. *Development* **122**, 627-635.

Steinberg, Z., Myers, C., Heim, V. M., Lathrop, C. A., Rebustini, I. T., Stewart, J. S., Larsen, M. and Hoffman, M. P. (2005). FGFR2b signaling regulates ex vivo submandibular gland epithelial cell proliferation and branching morphogenesis. *Development* **132**, 1223-1234.

Stevens, T. A. and Meech, R. (2006). BARX2 and estrogen receptor-alpha (ESR1) coordinately regulate the production of alternatively spliced ESR1 isoforms and control breast cancer cell growth and invasion. *Oncogene* **25**, 5426-5435.

Stevens, T. A., Iacovoni, J. S., Edelman, D. B. and Meech, R. (2004). Identification of novel binding elements and gene targets for the homeodomain protein BARX2. *J. Biol. Chem.* **279**, 14520-14530.

Villapando, I., Ramirez, M., Zepeda-Rodriguez, A., Castro, A. C., Cardenas-Vazquez, R. and Vilchis, F. (2005). The Harderian gland of the Mexican volcano mouse Neotomodon alstoni alstoni (Merriam 1898): a morphological and biochemical approach. *J. Exp. Zool. A Comp. Exp. Biol.* **303**, 13-25.

Wang, Y. L., Tan, Y., Satoh, Y. and Ono, K. (1995). Morphological changes of myoepithelial cells of mouse lacrimal glands during postnatal development. *Histol. Histopathol.* **10**, 821-827.

Weaver, M., Dunn, N. R. and Hogan, B. L. (2000). Bmp4 and Fgf10 play opposing roles during lung bud morphogenesis. *Development* **127**, 2695-2704.

Wiseman, B. S., Sternlicht, M. D., Lund, L. R., Alexander, C. M., Mott, J., Bissell, M. J., Soloway, P., Itohara, S. and Werb, Z. (2003). Site-specific inductive and inhibitory activities of MMP-2 and MMP-3 orchestrate mammary gland branching morphogenesis. *J. Cell Biol.* **162**, 1123-1133.

Zylberberg, C., Seamon, V., Ponomareva, O., Vellala, K., Deighan, M. and Azzarolo, A. M. (2007). Estrogen up-regulation of metalloproteinase-2 and -9 expression in rabbit lacrimal glands. *Exp. Eye Res.* **84**, 960-972.

Table S1. Correlation of eyelid and lacrimal gland (LG) phenotypes in *Barx2* null mice

Eye phenotype	LG phenotype				Total number of eyes studied
	Normal/slightly small	Small	Vestigial	Absence of LG	
Open eyelid eye surface inflammation	0	7	3	1	11
Normal eyelid closure (no inflammation)	4	2	0	0	6
Slit eye (internal eyelid surface fused with corneal surface)	0	0	1	6	7

Correlation of eye inflammation, eyelid and LG defects was studied in 3- to 6-month-old *Barx2* null mice.

Table S2. Expression of matrix metalloproteinases (MMPs) and tissue inhibitors of metalloproteinases (TIMPs) in separated lacrimal gland mesenchyme and epithelium

Protein	Epithelium	Mesenchyme
Barx2	++	–
Barx1	–	+++
Timp1	+	++
Timp2	++	+++
Timp3	–	+
Timp4	–	+
Mmp2	++	+++
Mmp3	–	++
Mmp9	+	++

+++, strong expression, ++, moderate expression, +, weak expression, –, no expression.

Lacrimal glands were obtained from E16.5 embryos and epithelium and mesenchyme were enzymatically separated and processed for quantitative RT-PCR as described in Materials and methods.